INTERNATIONAL JOURNAL OF ROBOTICS
(THEORY AND APPLICATIONS)
E-mail: IJR@kntu.ac.ir

On Passive Quadrupedal Bounding with Flexible Linear Torso

K. Koutsoukis [a], E. Papadopoulos [a,*]

[a] Department of Mechanical Engineering, National Technical University of Athens, Athens, Greece, 15780.

ARTICLE INFO

Article history:

Received: March 20, 2015.
Received in revised form:
July 31, 2015.
Accepted: August 28, 2015.

Keywords:

Legged robots
Passive quadruped
Flexible linear torso

ABSTRACT

This paper studies the effect of flexible linear torso on the dynamics of passive quadruped bounding. A reduced-order passive and conservative model with linear flexible torso and springy legs is introduced. The model features extensive spine deformation during high-speed bounding, resembling those observed in a cheetah. Fixed points corresponding to cyclic bounding motions are found and calculated using numerical return map methodologies. Results show that the corresponding robot gaits and the associated performance resemble those of its natural counterparts.

1. Introduction

Among the legged animals, quadrupeds are characterized by high-speed locomotion. The main mechanism for achieving such high-speeds is the increase of stride frequency; however there is an upper limit over which no further increase in frequency is possible [1]. To overcome this limitation, quadrupeds activate another mechanism, that of the compliant or flexible torso. Extensive flexion and extension of their torso is observed at high speeds only [1]. The cheetah, a natural elite sprinter, owes its astonishing performance in part to its flexible spine. Indeed, although the cheetah and the racing greyhound are of similar size and gross morphology, the cheetah attains significantly higher speed than the greyhound; the fastest recorded speed for the cheetah is $29 m/s^2$ [2] in contrast to a $17 m/s$ top speed for the racing greyhound [3]. Earlier studies in the context of fast quadruped locomotion have revealed the extensive use of spine by galloping mammals. Hildebrand studied the phases of a stride during cheetah galloping, and noted the extensive spine deformation and the large stride length of the cheetah, [4] and [5], see Fig. 1. According to studies focusing on the temporal and spatial characteristics of locomotion, the combination of large stride length and low stride frequency is considered the key to attaining high speed [6]. In addition to its contribution to speed, a flexible spine enhances energy efficiency by storing in elastic form the fluctuating energy due to the swinging of a quadruped leg, at the spine musculature elements, such as the aponeurosis of the longissimus thoracis et lumborum muscle [7].

In the last twenty years, scientists presuming the importance of the spine have developed a large number of dynamically stable quadruped robots with flexible torso, trying to enlist its benefits. Leeser introduced the first robot in this category [8], following Raibert's pioneering work [9]. It was a hydraulic planar robot with two telescoping springy legs and an articulated spine composed of three segments with actuated joints. Since then various spine implementations have been proposed, others with simple designs and others with more complex biomimetic designs.

*Corresponding address: E-mail address: egpapado@central.ntua.gr
tel: +30 210-772-1440 fax: +30 210-772-1455
This research has been financed by the European Union (European Social Fund – ESF) and Greek funds through the Operational Program "Education and Lifelong Learning" of the National Strategic Reference Framework (NSRF) – Research Program: ARISTEIA: Reinforcement of the interdisciplinary and/or inter-institutional research and innovation

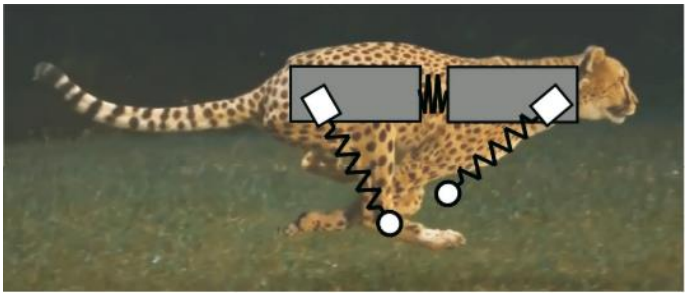

Figure 1. The sagittal model with a flexible linear spine overlayed a cheetah at the gathered flight phase in the background.

The Bobcat [10] robot and the Lynx modular robot [11] are representative examples of small quadruped robots with a simple spine implementation, since they feature one and multiple revolute spinal joints respectively. Some of the complex designs worth mentioning are the MIT Cheetah [12], and the Canid robot [13], both with flexible torsos consisting of intervertebral discs (flexible elements capable of storing elastic energy), and vertebrae (rigid braces supporting the intervertebral discs).

Other interesting spine implementations were introduced by the Renny robot with a ball-and-socket joint, and antagonistic pneumatic artificial muscles [14], and by the Tiger robot featuring a compliant spinal bending mechanism consisting of light-weight segments and a linear spring [15]. In general, the complexity of legged robots does not permit a generic analysis and insight of the effect of spine motions on quadruped locomotion, since most results and conclusions are highly depended on the implementation of the robot. So the need for reduced models of articulated spine robots has emerged.

In the literature, a variety of dynamic models have been proposed to study the influence of the articulated spine on quadrupedal running. In analogy to the Spring Loaded Inverted Pendulum (SLIP), the models have springy legs, which in most studies are massless [16-19], except for those in [20, 21]. The vast majority of the proposed models feature a rotary back joint, either actuated [19], [21] or passive [16-18], [20] with the single exception that of the one-dimensional model, which features a translational joint spine and oversimplified legs, i.e. the legs are represented as masses always in contact with the ground, moving due to controlled actuator-applied forces and to the difference between the forward and backward friction [22].

In this article, we introduce a sagittal plane model with a linear flexible torso and massless springy legs, to the best of our knowledge for the first time in the literature. The model is passive and conservative, but despite its simplicity, it allows the prediction of the existence of repetitive passive gaits corresponding to Poincaré fixed-points, and of resulting motions resembling those of its natural counterparts. The developed model is the only one that captures the extensive variation of the sagittal hip-to-hip distance due to spine deformation. This property has not been captured in other works so far, due to the use of a revolute spinal joint.

The structure of the paper is as follows. In Section 2, the model with the flexible linear torso is introduced and the equations of motion are presented. Section 3 discusses in detail the main properties of the calculated cyclic bounding motions realized passively. Section 4 concludes the paper.

2. Dynamics of bounding with flexible linear torso

A quadruped robot is a complex nonlinear system with hybrid dynamics, characterized by the strong coupling between many degrees of freedom. In order to study the effect of the flexible linear torso during fast locomotion, a simplified sagittal model of a quadruped robot is introduced, as shown in Fig. 2.

2.1. Model description and parameters

The main body of the model consists of two segments (hind and fore segments). The two segments of the body are connected via the spinal translational joint, which is passive, with a linear spring connecting the two body segments and which allows no rotation between them. Two springy legs are connected to each of the two body segments at the hips with revolute joints. The choice of springy legs is in analogy with the Spring Loaded Inverted Pendulum (SLIP) and captures the property of energy storage during running. Subscripts , , and , refer to the fore and hind individual body segments (or legs) and to the torso, respectively.

As far as the dynamics of the model is concerned, the hind and fore segments of the body are identical with mass and moment of inertia about their center of mass (CoM). The legs are massless springs of nominal length and spring stiffness, and the distance between the hip joint and the CoM of each body is.

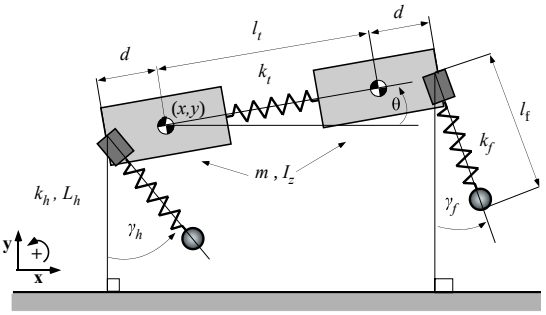

Figure 2. The sagittal-plane model of a quadruped robot with a linear flexible torso.

The spinal joint is a linear spring of stiffness and nominal length. The model is conservative since energy dissipation and motor input torques are not considered. The values of the model mechanical parameters are chosen to match the parameters in [17]. The value for the stiffness of the torso linear spring was chosen so that the herein introduced model and the model of [17] have the same natural frequency. The model mechanical properties are displayed in Table 1.

Table 1. Model Mechanical Properties

PARAMETER	VALUE	UNITS
Fore/hind body mass (m)	10.432	Kg
Fore/hind body inertia (I_z)	0.339	Kg M^2
Hip to com distance (d)	0.138	M
Nominal leg length (L)	0.323	M
Leg spring constant (k)	7046	N/M
Nominal torso spring length (L_t)	0.276	M
Torso spring stiffness (k_t)	5077	N/M

2.2. Bounding gait description

In nature, mammals use their spine mainly during high speed galloping [1], [4], [5]. Galloping is an asymmetric gait, featuring great complexity since none of the legs moves in phase with another. Instead in bounding, i.e. the gait at which the fore and the hind legs move in phase, is easier to model and is employed frequently in nature during obstacle avoidance and running with moderate speed. In the robotic community bounding has received considerable attention due to its sagittally symmetric nature and to its use as a limiting case of galloping.

In this paper, we study the spine performance during bounding. Bounding consists of four phases, two aerial and two stance phases triggered by events such as leg liftoff and leg touchdown. The phases of bounding are illustrated in Fig. 3. It is interesting to note the existence of two flight phases. During the gathered flight phase, the spine spring reaches its minimum length, letting the two body segments to approach. No collision is modeled, so the two CoMs can come as close as needed. During the extended flight phase, the spinal spring reaches its maximum length, increasing the distance between them.

The existence of a fifth phase, called double stance phase, during which the two legs are in contact with the ground simultaneously, is also possible. In such a case, the double stance replaces the gathered flight phase; however this type of bounding is not studied here.

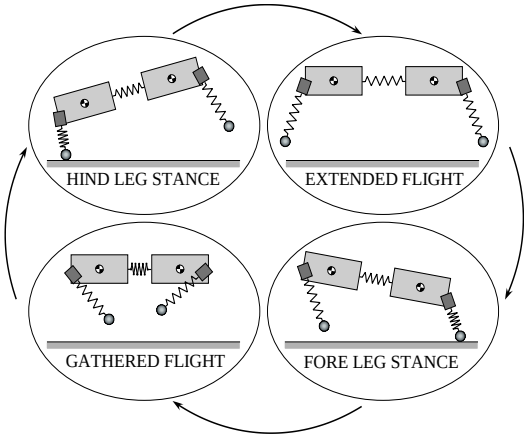

Figure 3. Bounding phases and events.

2.3. Equations of motion

The equations of motion are derived using the Lagrangian formulation. Virtual legs are used, i.e. the fore or hind leg pairs that move together, are replaced by a single leg with double stiffness. The generalized coordinates include the Cartesian coordinates of the CoM of the hind segment, the pitch angle of the body and the spinal spring length i.e. the distance between the CoMs of the two body segments. Assuming that during stance, the foot-ground contact acts as a pin joint and no slippage occurs, the leg lengths (l_f , l_h) and the absolute leg angles with respect to the vertical to the ground (γ_f , γ_h) , can be expressed using the generalized coordinates as:

$$l_f = \sqrt{[y + (l_t + d)\sin\theta]^2 + [x_{tdf} - x - (l_t + d)\cos\theta]^2} \quad (1)$$

$$l_h = \sqrt{(y - d\sin\theta)^2 + (x_{tdh} - x + d\cos\theta)^2} \quad (2)$$

$$\gamma_f = \tan^{-1}\left(\frac{x_{tdf} - x - (l_t + d)\cos\theta}{y + (l_t + d)\sin\theta}\right) \quad (3)$$

$$\gamma_h = \tan^{-1}\left(\frac{x_{tdh} - x + d\cos\theta}{y - d\sin\theta)}\right) \quad (4)$$

where x_{tdf} and x_{tdh} is the x coordinate of the foot at fore and hind leg touchdown events respectively, and remain constant during the stance phase.

Using (1) - (4), the equations of motion can be simplified. Defining as $\mathbf{q} = [x \quad y \quad \theta \quad l_t]^T$ the equations of motion can be written in matrix form as:

$$\mathbf{M(q)}\ddot{\mathbf{q}} = \mathbf{F(q,\dot{q})} + \mathbf{G(q)} \tag{5}$$

where **M** is the mass matrix, the vector **F** contains the Coriolis, the centrifugal and the leg forces acting on the bodies, and the vector **G** contains the gravitational terms, and are given below:

$$\mathbf{M(q)} = \begin{bmatrix} 2m & 0 & -ml_t\sin\theta & m\cos\theta \\ 0 & 2m & ml_t\cos\theta & m\sin\theta \\ -ml_t\sin\theta & ml_t\cos\theta & 2I_z + ml_t^2 & 0 \\ m\cos\theta & m\sin\theta & 0 & m \end{bmatrix} \tag{6}$$

$$\mathbf{F(q,\dot{q})} = \begin{bmatrix} 2m\dot{\theta}\dot{l}_t\sin\theta + m\dot{\theta}^2 l_t\cos\theta + F_h\sin\gamma_h + F_f\sin\gamma_f \\ -2m\dot{\theta}\dot{l}_t\cos\theta + m\dot{\theta}^2 l_t\sin\theta + F_h\cos\gamma_h + F_f\cos\gamma_f \\ -2m\dot{\theta}\dot{l}_t l_t + F_f(\mathrm{d}+l_t)\cos(\theta-\gamma_f) - F_h\mathrm{d}\cos(\theta-\gamma_h) \\ k_t(L-l_t) + m\dot{\theta}^2 l_t + F_f\sin(\theta-\gamma_f) \end{bmatrix} \tag{7}$$

$$\mathbf{G(q)} = \begin{bmatrix} 0 \\ -2mg \\ -mgl_t\cos\theta \\ -mg\sin\theta \end{bmatrix} \tag{8}$$

and

$$F_f = k(L - l_f) \tag{9}$$

$$F_h = k(L - l_h) \tag{10}$$

The leg forces are zero when a leg does not touch the ground.

2.4. Events and phase transition

The dynamics of the model is hybrid, containing terms that are activated and deactivated depending on the phase of bounding. Of major importance are the conditions under which an event occurs and triggers the phase transition for the model. The touchdown and liftoff events, as well as the phase transitions are described below.

1) Touchdown events: The flight phase terminates when the lower part of the leg touches the ground. Using the absolute angles (γ_f, γ_h) of the leg and Cartesian coordinates of the hind segment of the body, the criterion for the touchdown event to occur for the hind leg is:

$$y - d\sin\theta - L\cos\gamma_h = 0 \tag{11}$$

accordingly, the criterion of the fore leg touchdown is:

$$y + (d + l_t)\sin\theta - L\cos\gamma_f = 0 \tag{12}$$

2) Liftoff events: The stance phase terminates when the ground reaction force becomes zero and the leg acceleration is positive i.e. the leg and consequently the segment to which it is attached is moving upwards. Under the assumption of massless legs, the liftoff threshold is significantly simplified since the liftoff occurs when a spring leg reaches its nominal length. The threshold function for the fore leg liftoff is:

$$l_f - L = 0 \tag{13}$$

accordingly, the liftoff criterion for the hind leg is:

$$l_h - L = 0 \tag{14}$$

2.5. Bounding cyclic motions

To study the existence of bounding cyclic (repetitive) motions as shown in Fig. 3, the method of the Poincaré return map is employed. The Poincaré section is taken in the extended flight phase at the apex height of the spinal joint, where the vertical velocity of the CoM of the total body (consisting of the two segments) is zero, that is:

$$2\dot{y} + \dot{l}_t\sin\theta + \dot{\theta}l_t\cos\theta = 0 \tag{15}$$

To study the periodic motions through the computations of *fixed-points* on a Poincaré map, the monotonically increasing horizontal coordinate x of the CoM of the hind segment of the body will be projected out of the state vector. A further dimensional reduction inherent to the Poincaré method can be employed to substitute $\dot{y}$, θ and $\dot{l}_t$. The reduced Poincaré map can be defined through the rule,

$$\mathbf{z}_f[k+1] = \mathbf{P}(\mathbf{z}_f[k],\ \mathbf{a}_f[k]) \tag{16}$$

where

$$\mathbf{z}_f = (y,\ \dot{\theta},\ \dot{x},\ l_t)^T \tag{17}$$

and

$$\mathbf{a}_f = (\gamma_f,\ \gamma_h)^T \tag{18}$$

includes the leg angles which are controlled kinematically.

3. Passive periodic motions

In this section, the search method for the passively generated fixed points and their main characteristics are presented. The objective is to find an argument $\mathbf{z}_f$ that maps onto itself i.e. the solution to the equation

$$\mathbf{z}_f[k+1] - \mathbf{P}(\mathbf{z}_f[k],\ \mathbf{a}_f[k]) = 0 \tag{19}$$

The search for fixed points was conducted in two levels. At the first level, possible areas of existence of fixed points were found, based on a rough search of initial conditions. At the second level, a search on the specified areas was conducted using MATLAB's *fmincon* and *patternsearch*. The results were filtered in order to discard from the sum of the calculated fixed points, the motions featuring double stance phase, since the resulting motion would have been in contrast to the bounding regime described in Section 2. Following this method, a large amount of fixed points has been computed.

The fixed point parameters, i.e. the initial spine deformation, the initial pitching rate and the initial forward velocity, and the initial vertical distance of the ground, vary significantly. However some basic properties characterize the vast majority of fixed-points. To study the effect of the flexible linear torso to the bounding motion, we focus next to a representative fixed point.

Figures 4 to 6 illustrate the evolution of the main variables of motion corresponding to a representative fixed point derived with the initial conditions given in Table 2 The motion produced with these initial conditions is characterized by a high-speed bounding (i.e. of 4.3 m/s, as shown in Fig. 4b) featuring extensive bidirectional spine deformation and reduced pitching motion.

Table 2. Fixed point initial conditions and Touchdown angles

VARIABLE	VALUE	UNITS
Horizontal Velocity of hind body CoM $(\dot{x})$	4.3	m/s
Vertical Position of hind body CoM (y)	0.3	m
Pitch Rate $(\dot{\theta})$	-119.0	deg/s
Spine Spring Length (l_t)	0.35	m
Fore Leg Touchdown angle (g_f)	26.0	deg
Hind Leg Touchdown angle (g_h)	25.0	deg

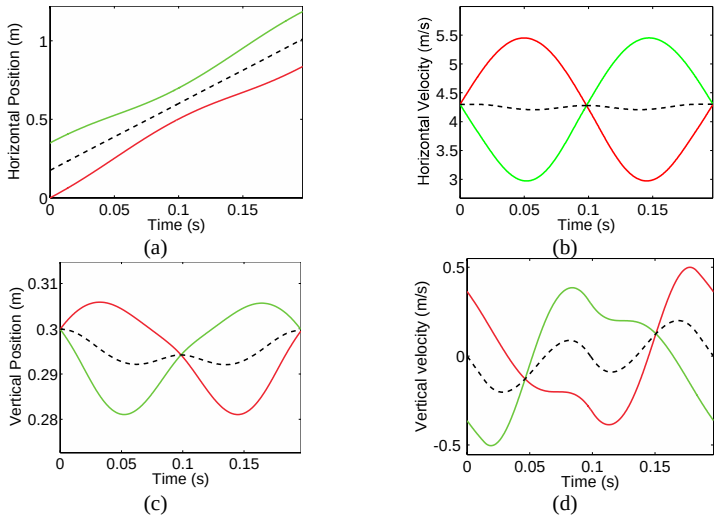

Figure 4. Time evolution of the Cartesian variables for the CoM of fore body segment (solid green), hind body segment (solid red) and whole system (dashed black) at a representative passively generated fixed point during bounding. (a) horizontal body positions, (b) horizontal velocity, (c) vertical position, (d) vertical velocity.

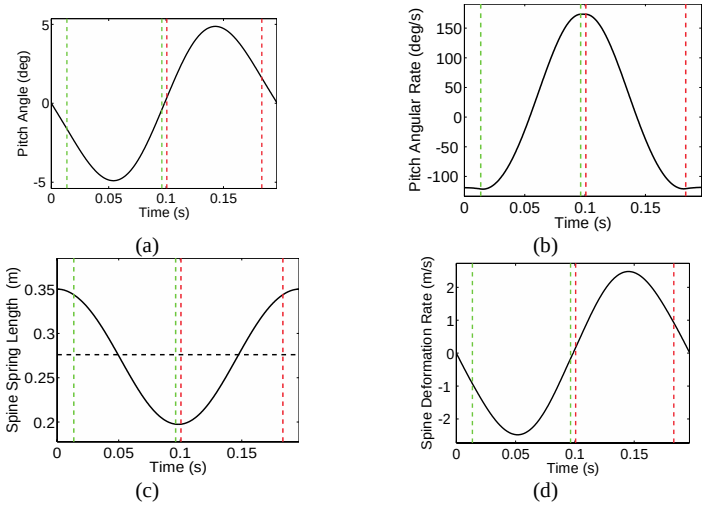

Figure 5. Evolution of the pitch angle, pitch rate, spine linear deformation and spine linear deformation rate with respect to time at a representative passively generated fixed point. The vertical dashed lines correspond to touchdown and liftoff events related to fore legs (green dashed line) and to hind legs (red dashed line). The spine spring nominal length is represented by the dashed black line.

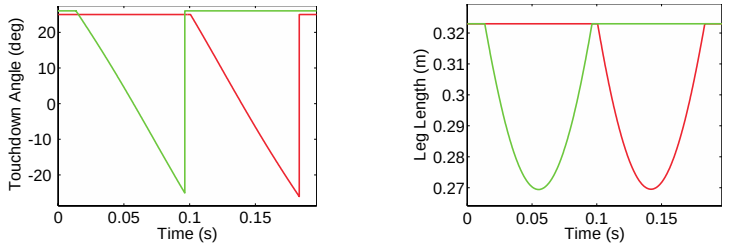

(a) (b)

Figure 6. Evolution of the absolute leg angles (with respect to the vertical of the ground) and the leg length for the fore (solid green line) and the hind (solid red line) with respect to time.

At the start of the bounding cycle, the robot is placed at the apex height of the spinal joint, where the vertical velocity of the system CoM is zero. The spinal spring is extended reaching its maximum deformation, and the legs have their proper touchdown angles. The free fall of the robot ends with the fore leg touchdown and the system enters the fore stance phase. Under the impact of the contact force, the fore leg spring deforms. When it reaches its nominal length, the fore liftoff event occurs. After the gathered flight phase at which the maximum flexion of the spine spring appears, the same sequence of events repeats for the hind legs. Following the hind leg liftoff, the model returns to the apex height of the spinal joint, completing a stride. The aforementioned cyclic motion exhibits some characteristics worth mentioning.

As far as the spine motion is concerned, during the bounding stride the spinal spring features extensive bidirectional deformation. In more detail, the maximum flexion and the maximum extension of the spring exceeds 25% of its nominal length resulting to a large variation of the distance between the fore and the hind hip. This characteristic is in agreement with the extensive body length variation of galloping mammals [4], [5]. In addition the maximum spinal flexion and extension occur before and after hind and fore touchdown events respectively and are not strictly coupled to the events, as described also in recent research concerning therian mammals. [23]. Another interesting result is the low amount of spine elastic energy needed to produce the cyclic bounding motion, see Fig. 7.

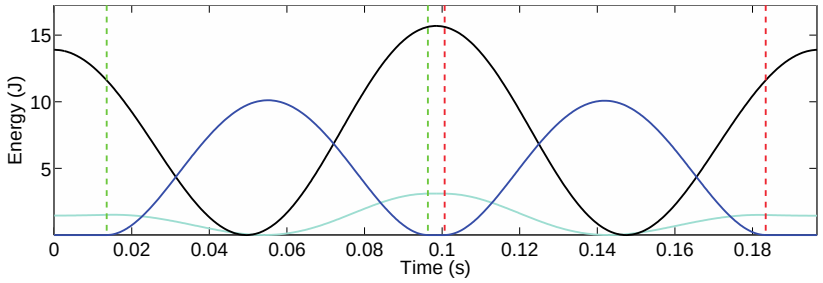

Figure7. Evolution of spine energy (black line), leg deformation energy (blue line) and angural kinetic energy (cyan line) with respect to time at the representative fixed point. The vertical dashed lines correspond to touchdown and liftoff events related with fore legs (green dashed line) and the hind legs (red dashed line). The spine spring nominal length is represented by the dashed black line.

The motion of the linear torso model at the representative fixed point possesses another interesting characteristic in terms of the horizontal velocity of its body segments. During the repetitive bounding gait, the extensive linear motion in Fig. 5c, and the relative small pitch angle in Fig. 5a, result in a large horizontal velocity variation between the fore and hind body segments while the horizontal velocity of the system CoM in Fig. 4b remains almost constant during the stride. Note that for each stance phase, the forward velocity of the segment in touch with the ground is significantly lower than the forward velocity of the system CoM.

Careful inspection of Fig. 4 reveals that the evolution of both velocities (vertical and horizontal) of the fore body segment, forward in time, is indistinguishable from the evolution of velocities of the hind body segment. Symmetry can be found also between the fore and hind leg touchdown and liftoff angles, where the absolute touchdown angle of the fore leg equals to the negative of the absolute liftoff angle of the hind leg, see Fig. 6a. The aforementioned time-reversal symmetry is a byproduct of the model symmetric properties of fixed points for the energy-preserving system, and also exists in the rotational spine model [17].

As a closing remark, it is worth mentioning that the gathered flight phase during bounding with a flexible linear torso is of relatively short duration, see Fig. 5 and Fig. 6. This fact results in a larger stance phase in comparison to the flexible revolute torso [17]. However, recent research on galloping mammals reveals that stance duration of high-speed galloping (rotary galloping) during which spine motions are observed, is larger than the stance duration of moderate speed galloping (transverse galloping), during which the spine motion is relatively small [1].

4. Conclusion

In this paper, the effect of linear flexible torso during high-speed galloping was investigated by introducing a planar reduced model featuring a linear spinal joint. Passive cyclic motions were discovered and calculated using the Poincaré return map. The properties of a representative fixed point corresponding to high velocity bounding were analyzed in detail. The quadrupedal bounding produced in the presence of a linear flexible torso, despite the reduced nature of the model, resembles the motion of galloping mammals and features extended bidirectional spine deformation.

References

[1] L. D. Maes, M. Herbin, R. Hackert, V. L. Bels, and A. Abourachid, Steady locomotion in dogs: Temporal and associated spatial coordination patterns and the effect of speed, Journal of Experimental Biology, Vol. 211, (2008), 138–149.

[2] N. Sharp, Timed running speed of a cheetah (Acinonyx jubatus), Journal of Zoology. Vol. 241, (1997), 493-494

[3] J. R. Usherwood, A. M. Wilson, Biomechanics: no force limit on greyhound sprint speed, Nature, Vol. 438, (2005), 753-754.

[4] M. Hildebrand, Motions of the running cheetah and horse, Journal of Mammalogy, Vol. 40(4), (1959), 481–495.

[5] M. Hildebrand, Further studies on locomotion of the cheetah, Journal of Mammalogy Vol. 42(1), (1961), 84–91.

[6] P. E. Hudson, S. A. Corr and A. M. Wilson,, High speed galloping in the cheetah (Acinonyx jubatus) and the racing greyhound, (Canis familiaris): spatio-temporal and kinetic characteristics, Journal of Experimental Biology, Vol. 215, (2012), 2425-2434.

[7] R.M. Alexander, N.J. Dimery and R.F. Ker, Elastic structures in the back and their role in galloping in some mammals, Journal of Zoology, Series A, Vol. 207, (1985), 467–482.

[8] K. F. Leeser, Locomotion Experiments on a Planar Quadruped Robot with Articulated Spine. Master thesis, Massachusetts Institute of Technology, (1996).

[9] M. H. Raibert, Legged Robots that Balance. Cambridge, MA: MIT Press, (1986).

[10] M. Khoramshahi, A. Spröwitz, A.Tuleu, M. N. Ahmadabadi and A. J. Ijspeert, Benefits of an Active Spine Supported Bounding Locomotion With a Small Compliant Quadruped Robot, in Proceedings of the IEEE International Conference on Robotics & Automation (ICRA), Karlsruhe, (2013), 3329–3334.

[11] P. Eckert, A. Sprowitz1, H. Witte and A. J. Ijspeert, Comparing the effect of different spine and leg designs for a small bounding quadruped robot, in Proceedings of the IEEE International Conference on Robotics & Automation (ICRA), Seattle, (2015), 3128-3133.

[12] S. Seok, A. Wang, M. Y. Chuah, D. Otten, J. Lang, and S. Kim, Design principles for highly efficient quadrupeds and implementation on the MIT cheetah robots, in Proceedings of the IEEE International Conference on Robotics and Automation, Karlsruhe, (2013), 3307–3312.

[13] G. C. Haynes, J. Pusey, R. Knopf, A. M. Johnson and D. E. Koditschek, Laboratory on Legs: An Architecture for Adjustable Morphology with Legged Robots, in Proceedings of the SPIE Defense, Security, and Sensing Conference, Unmanned Systems Technology XIV, (2012).

[14] Q. Zhao, B. Ellenberger, H. Sumioka, T. Sandy and R. Pfeifer, The Effect of Spine Actuation and Stiffness on a Pneumatically-driven Quadruped Robot for Cheetah-like Locomotion, in Proceeding of the IEEE International Conference on Robotics and Biomimetics (ROBIO), Shenzhen, China, (2013), 1807-1812.

[15] J. Bidgoly, A. Vafaei, A. Sadeghi, M. N. Ahmadabadi, Learning approach to study effect of flexible spine on running behavior of a quadruped robot, in Proceedings of the 13th International conference on Climbing and Walking Robots and the Support Technologies for Mobile Machines, Nagoya, (2010).

[16] J. E. Seipel, Analytic-holistic two-segment model of quadruped back-bending in the sagittal plane, in Proceedings of ASME International Design Engineering Technical Conferences & Computers and Information in Engineering Conference, Washington, (2011), 855-861.

[17] Q. Cao, I. Poulakakis, Passive quadrupedal bounding with a segmented flexible torso, in Proceedings of the IEEE/RSJ International Conference on Intelligent Robots and Systems, Algarve, (2012), 2484–2489.

[18] G. C. Haynes, Dynamic bounding with a passive compliant spine, in Proceedings of the Dynamic Walking Conference, (2012).

[19] Q. Deng, S. Wang, X. W., J. Mo, and Q. Liang, Quasi passive bounding of a quadruped model with articulated spine, Mechanism and Machine Theory, Vol. 52, (2012), 232–242.

[20] Q. Cao, I. Poulakakis, On the Energetics of Quadrupedal Bounding With and Without Torso Compliance, in Proceedings of the IEEE/RSJ International Conference on Intelligent Robots and Systems, Chicago, (2014), 4901-4906.

[21] U. Culha, U. Saranli, Quadrupedal Bounding with an Actuated Spinal Joint, in Proceedings of the IEEE International Conference on Robotics and Automation, Shanghai, China, (2011), 1392-1397.

[22] M. Khoramshahia, H. J. Bidgoly , S. Shafiee, A. Asaei, A.J.Ijspeert , M. N. Ahmadabadia, Piecewise linear spine for speed–energy efficiency trade-off in quadruped robots, Robotics and Autonomous Systems, Vol. 61(12), (2013), 1350-1359.

[23] N. Schilling, R. Hackert, Sagittal Spine Movements of Small Therian Mammals during Asymetrical Gaits, Journal of Experimental Biology, Vol. 209, (2006), 3925–3939.

[24] I. Poulakakis, E. Papadopoulos, and M. Buehler, On the Stability of the Passive Dynamics of Quadrupedal Running with a Bounding Gait, The International Journal of Robotics Research, Vol. 25(7), (2006), 669–687.

Biography

Konstantinos Koutsoukis received his Diploma in Mechanical Engineering from the National Technical University of Athens (NTUA) in 2012. He is currently a Ph.D. candidate in the Department of Mechanical Engineering of NTUA and a research assistant with the Control Systems Laboratory (CSL). His research interests include system dynamics, design and control of robotic systems, and legged robots. He is a Member of the Technical Chamber of Greece.

Evangelos Papadopoulos received his Diploma from the National Technical University of Athens (NTUA) in 1981, and his M. S. and Ph.D. degrees from MIT in 1983 and 1991 respectively, all in Mechanical Engineering. He was an analyst with the Hellenic Navy, Athens, Greece, from 1985 to 1987. In 1991 he joined McGill U. and the Centre for Intelligent Machines (CIM) as an Assistant Professor. Currently, he is a Professor with the Department of Mechanical Engineering at the NTUA.

He teaches courses in the areas of Systems, Controls, Mechatronics and Robotics. His research interests are in the area of robotics, modeling and control of dynamic systems, mechatronics and design. He serves as an Associate Editor for the *ASME J. of Dynamic Systems, Measurement and Control,* the *IEEE Robotics and Automation Letters (RA-L),* and the *Machine and Mechanism Theory*, while previously he served as an Associate Editor of the *IEEE Transactions on Robotics,* and as a Guest Editor for the *IEEE/ASME Transactions on Mechatronics*. He has published more than 240 technical articles in journals and refereed conference proceedings. He is a Senior Member of AIAA and a Member of the ASME, of the Technical Chamber of Greece and of Sigma Xi.